Probing the Hydrodynamic Behavior of Drug-Induced Tubulin Rings by Fluorescence Correlation Spectroscopy

Hacène Boukari, Dan L. Sackett, Ralph Nossal*

Laboratory of Integrative and Medical Biophysics, National Institutes of Health, Bethesda, MD 20892, USA
Email: boukarih@mail.nih.gov; sackettd@mail.nih.gov; rjn@helix.nih.gov

Summary: We describe fluorescence correlation spectroscopy measurements of tubulin polymers composed of tubulin and either of two cytotoxic peptides – dolastatin 10 and cryptophycin 1. These peptides inhibit tubulin polymerization into microtubules, a major component of cellular networks, and instead induce the formation of predominantly single-walled tubulin rings. We determine ratios of the hydrodynamic diameter of dolastatin-tubulin or cryptophycin-tubulin polymers to that of tubulin dimers, which are compared with corresponding ratios calculated for two simple models: 1) a circular ring made with N contiguous spherical beads and 2) a circular ring constructed with N non-spherical monomers, each monomer being represented by 21-minibeads. We find that the computed ratios from the 21-minibead representation agree well with the measured ones when N = 28 and N = 16 for dolastatin-tubulin and cryptophycin-tubulin ring polymers, respectively. That is, the rings are made with 14 and 8 tubulin dimers, confirming the numbers derived by other techniques. The present results further support the applicability of theories that have been developed for calculating hydrodynamic properties of supramolecular biological structures.

Keywords: cryptophycin; dolastatin; fluorescence correlation spectroscopy; microtubules; tubulin rings

Introduction

Microtubules are hollow cylindrical polymers built from the heterodimeric proteins, $\alpha\beta$-tubulin (MW $\approx$ 100 kDa)[1,2]. In eukaryotic cells they form a dynamical network that performs important cellular functions such as protein trafficking and cell division[1]. Disruption or alteration of this network and/or its functions can provide a therapeutic route by which cancerous cells can be targeted. Vinblastine and Taxol are examples of chemical compounds that affect microtubule activities and have been developed into clinically useful anti-cancer agents[3,4] (see also references therein). Details of the mechanism(s) of these anti-microtubule activities are not well understood. In vitro, various experimental investigations indicate that the binding of these chemical compounds results in significant structural changes, ranging from hyperstabilization of microtubules (loss of reversible polymerization-

 DOI: 10.1002/masy.200550921

depolymerization), to complete depolymerization of microtubules, to induction of aberrant non-microtubule polymers.

Recently, a new class of small peptides (cryptophycin, dolastatin, hemiasterlin, ...), which are extracted from marine products, has been shown to exhibit potent cytotoxicity (for review, see Reference 4). In solutions, these peptides appear to bind to the same location on tubulin and tend to depolymerize microtubules, causing the tubulin dimers to assemble into closed, single-walled, ring-like nanoscopic structures[4,5]. Cryo-electron microscopy revealed that the predominant cryptophycin-induced ring is composed of eight dimers[5], having a diameter of about 24 nm[5]. In References 6–8, we described results of analysis of fluorescence correlation spectroscopy (FCS), sedimentation velocity (SV), and small-angle neutron scattering (SANS) measurements, which indicate that the cryptophycin-tubulin rings appear rigid, have well-defined circular geometry, are highly monodisperse in size (8 dimers per ring), and are stable against dilution to nanomolar concentrations.

In contrast, dolastatin-tubulin polymer rings have a diameter of about 44 nm[4]. Moreover, at micromolar tubulin concentrations, the rings assemble into much larger entities that settle into the bottom of the sample container. SANS data indicate that these assemblies are likely cylinders formed by stacking of the rings[7]. As the concentration is lowered, FCS measurements show that the rings tend to depolymerize, especially below 10 nM concentration[6].

In this paper, we describe FCS measurements of dolastatin-tubulin (DoTu) solutions and compare them with those of cryptophycin-tubulin (CrTu) solutions. While FCS measurements on CrTu samples indicate a narrow dispersity in ring size, the DoTu samples appear polydisperse and the FCS data are better fit with an expression for two components (free tubulin dimers and polymerized tubulin). This fit yields an apparent hydrodynamic diameter for the second DoTu component (~ 31 nm), larger than that of the CrTu rings (~ 20 nm) and confirming the difference between the two tubulin polymers. Further, hydrodynamic modeling shows that the number of tubulin dimers per ring is 8 and 14 for CrTu and DoTu rings, respectively. Here, we follow the approach described in Reference 6, in which we compare the ratio of the measured diffusion time of the drug-induced polymer and that of the primary tubulin dimers (Tu) with the corresponding ratio calculated for two structural models: rings made with N spherical beads and rings made with N non-spherical monomers. These monomers are constructed with 21-minibeads, spatially distributed such that the non-spherical nature of the tubulin monomer is well represented[2,10].

Materials

MAP-free cow brain tubulin, labeled with an average of about 1 tetramethylrhodamine fluorophore per dimer, was obtained from Molecular Probes. Cryptophycin-1 (MW = 700 Da) was a kind gift from Dr. Susan Mooberry, Cancer Research Center of Hawaii. Dolastatin-10 (MW = 785 Da) was supplied by Dr. Robert Schultz, Drug Synthesis and Chemistry Branch, National Cancer Institute, Bethesda, Maryland. All other chemicals were purchased from Sigma Chemicals, St. Louis, Missouri.

The drug-tubulin samples were prepared as follows. First, tubulin (5 μM) and drug (8 μM) were mixed in PIPES buffer (0.1 M PIPES, 1 mM $MgCl_2$, pH 7.0) to initiate ring polymerization and to assure structural stability as observed and characterized by other techniques[5]. Then, the drug-tubulin solution was diluted in PIPES buffer, supplemented with 0.1 mg/ml of Bovine Serum Albumin (BSA), to a lower nominal concentration (100 nM) and filtered through a 0.22 μm pore filter. The added BSA helps reduce interaction of tubulin with the walls of the sample holder. Samples were loaded into 60 μl chambers (Grace Bio-Labs, Inc., Bend, Oregon, USA), whose bottom windows are made of glass coverslips. All measurements were made at room temperature (22 °C).

Fluorescence Correlation Spectroscopy

Our experimental FCS setup is described elsewhere[6]. FCS utilizes temporal fluctuations in fluorescence intensity to obtain information about particle motions occurring within a small excitation volume[11-15]. Fluorescence intensities, $I(t)$, acquired sequentially at times, t, are time-correlated to generate a correlation function defined as:

$$G(\tau) = 1 + \frac{<\delta(t)\delta(t+\tau)>}{<I(t)>^2} \quad , \quad (1)$$

where $\delta(t) = I(t) - <I(t)>$ denotes the deviation of the measured intensity from the average intensity, $<I(t)>$. The excitation volume is made small (femtoliter to sub-femtoliter) by either confocal geometry or by multiphoton excitation[11]. Typically, samples containing nanomolar concentrations of particles are probed. For non-interacting, freely diffusing, fluorescent particles with different translational diffusion coefficients and brightness, a closed-form expression of Equation 1 was derived[14,15]:

$$G(\tau) = 1 + \frac{1}{\left[\sum_j N_j Q_j\right]^2} \sum_i \frac{N_i Q_i^2}{\left(1 + \frac{\tau}{\tau_{di}}\right)\left(1 + p\frac{\tau}{\tau_{di}}\right)^{0.5}} \qquad (2)$$

In Equation 2 N_i denotes the average number of fluorescent particles of type i in the excitation volume, Q_i the fluorescence quantum yield of the particles, and τ_{di} the diffusion time of the particles as defined below. In the derivation of Equation 2 it is assumed that the fluorescent particles are excited by a 3-dimensional gaussian beam, $W(r,z) = Ae^{-2(r/r_0)^2} e^{-2(z/z_0)^2}$, characterized by two length scales, r_0 and z_0, defined in the focusing plane and the optical axis along the direction of the laser beam, respectively. With such a gaussian beam, $\tau_{di} = r_0^2 / 4D_i$, D_i being the translational diffusion coefficient. Also, in Equation 2 $p = (r_0 / z_0)^2$ is an instrumental constant set by the width of the incident beam and the size of the confocal pinhole. Finally, we apply the Stokes-Einstein relation, $D_i = k_B T / 3\pi\eta d_{Hi}$, to determine the hydrodynamic diameter, d_{Hi}; k_B, T, and η are the Boltzmann constant, the temperature of the sample, and the viscosity of the solvent.

Results

In Figure 1 we compare count histories (scaled by the average count) measured from tubulin (Tu), cryptophycin-tubulin (CrTu), and dolastatin-tubulin (DoTu) samples which had a nominal 100 nM tubulin concentration. All measurements were taken under the same experimental conditions (bin time = 100 ms, T = 22 °C, laser power, identical microscope objective, identical pinholes,..etc). Compare the spread of the intensities, which is related to the average number of particles; the larger the spread, the smaller the number of particles. The spread in the count history of the CrTu sample appears larger than that of the Tu sample, indicating a reduction of the number of particles due to polymerization of the primary tubulin dimers. The uniform spread of the count histories of the Tu and CrTu samples indicates a uniform distribution of the particle sizes. The history of the DoTu sample shows, however, occasional spikes that can be attributed to entities much larger than the polymer rings. These entities were not removed by the filter (0.2 μm) although the average fluorescence intensity dropped by almost half after filtering.

In Figure 2 we plot correlation functions measured from the same samples. For each sample the fluctuating signal was correlated over a 10 to 40 minute time period. The changes of the amplitude, $[G(\tau \to 0)-1]$, which is inversely proportional to the average number of fluorescent particles in the excitation volume (see Equation 2), are consistent with the effects of polymerization, corrected for the reduction of the amount of tubulin due to filtering[8]. A better quantitative assessment of the polymerization is depicted in the inset of Figure 2, where we plot the correlation functions normalized to unity, $[G(\tau)-1]/[G(\tau \to 0)-1]$. This inset shows shifts of the diffusion time to longer times upon the polymerization of the tubulin dimers. The CrTu correlation curve is shifted uniformly with respect to that of the Tu curve, indicating a uniform change of the size from tubulin to tubulin polymers. That is, the size distribution of the CrTu polymers is relatively narrow, which is confirmed by the markedly good fit of the data with an expression for one-component system (see Equation 2). We include in Figure 2 the fitting curves of the Tu and CrTu data determined by nonlinear least-squares fitting of the measured correlation data and determine that $\tau_d(\text{CrTu})/\tau_d(\text{Tu}) = 2.75$.

However, the DoTu curve is not shifted uniformly with respect to the Tu curve, suggesting polydispersity of the sample. In principle, one needs to extract the appropriate distribution of τ_{di} (hence distribution of sizes) from the correlation function, a challenging mathematical inversion problem[15,16]. For simplicity, however, we assume the DoTu sample to be composed of two main components, tubulin dimers and oligomers (likely rings), and perform a nonlinear least-squares fit of the DoTu data with an expression for two components (Equation 2) with three fitting parameters, since the diffusion time of tubulin is fixed. We determine the following ratio of the diffusion times: $\tau_R/\tau(\text{Tu}) = 4.51$, τ_R being the diffusion time of the second component. It should be noted that the presence of a small number of larger entities (see spikes in Figure 1) introduces a small systematic deviation in the fit at longer times ($\tau > 10^4$ μs).

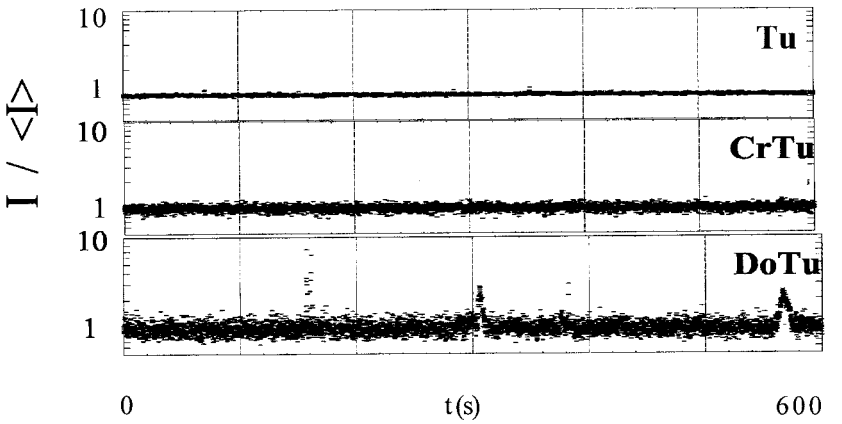

Figure 1. Time fluctuations of fluorescence intensities of rhodamine-labeled tubulin (Tu), cryptophycin-tubulin (CrTu), and dolastatin-tubulin (DoTu) samples normalized with respect to the corresponding time averages. Note the differences in the spread in intensities caused by the polymerization of tubulin into polymer rings when either cryptophycin or dolastatin is mixed with the tubulin samples. The spikes in the DoTu sample are caused by an additional assembly of the rings into larger entities (see text).

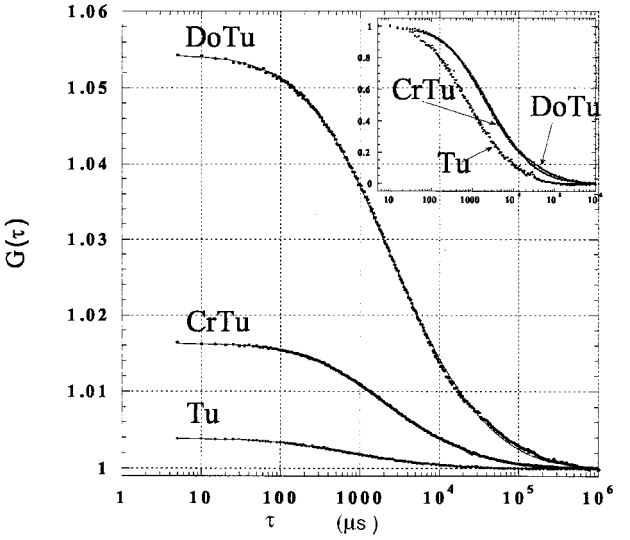

Figure 2. Measured correlation functions and fitted curves of rhodamine-labeled tubulin (Tu), cryptophycin-tubulin (CrTu), and dolastatin-tubulin (DoTu) samples are shown as a function of the delay time, τ. The inset, which shows the same data but normalized to unity, indicates the shift in the diffusion time caused by the polymerization of the tubulin dimers when mixed with cryptophycin or dolastatin.

For hydrodynamic modeling we first assume the basic tubulin monomer to be a spherical bead with diameter a. In this case, tubulin is represented as a dimer of beads and the tubulin ring is a rigid planar ring structure formed by N contiguous beads. Analytical expressions of the translational diffusion coefficient or, alternatively, the hydrodynamic diameter of both the dimer of beads and the N-bead ring have been derived[9,17]. The hydrodynamic diameter for the dimer is given by d_H(dimer) = 1.437a, where Stokes' law is assumed for an individual bead. For the N-bead ring, Yamakawa and Yamaki used the modified Riseman-Kirkwood approximation to determine the translational diffusion tensor. They showed that the tensor contains two diffusion coefficients, $D_{\parallel}$ along the plane of the ring and $D_{\perp}$ perpendicular to the plane, which are expressed by Equations (70) and (71) in Reference 9. The average diffusion coefficient was derived to be $D_N = (2D_{\parallel} + D_{\perp})/3 = k_B T / 3\pi\eta d_{HN}$, where d_{HN} denotes the hydrodynamic diameter of the N-bead ring. We plot in Figure 3 the calculated ratio, d_H(ring)/d_H(dimer), as a function of the number of beads, in which the dependence on the diameter cancels out. In addition, we include in the same plot the measured ratios of the diffusion times for the CrTu and DoTu samples, which are equivalent to the ratios of the hydrodynamic diameters when the Stokes-Einstein equation applies.

Although the values of the measured diffusion ratios in Figure 3 are within 6% (CrTu) and 12% (DoTu) of the values computed for the bead ring model, both appear lower than the calculated curve. Part of this relatively small discrepancy may be due to the fact that the dimer is hydrated on all surfaces, whereas water molecules are excluded from the interfaces between the dimers constituting the rings. Offsetting this effect is a possible expansion of the ring diameter due to the intercalation of the cryptophycin or dolastatin molecules. More likely, though, is that the asymmetric shape of the tubulin monomer is not adequately represented by the analytical expressions discussed in the preceding paragraph. Perhaps a more appropriate model is the 21-minibead representation of the tubulin monomer developed by Diaz et al. from small angle X-ray scattering data[10]. This model appears to capture more details of the actual nonspherical 3- dimensional shape of the tubulin monomer[2]. Again the tubulin dimer is represented by two contiguous 21-minibead monomers and the ring is constructed by assembling N 21-minibead monomers around a planar circle. Because of the complex configuration of the 21 minibeads, we apply the generic code, HYDRO[18,19], to compute the corresponding hydrodynamic diameters of the dimers and the ring as a function N. Here we set the individual bead radii to 1.3 nm, as

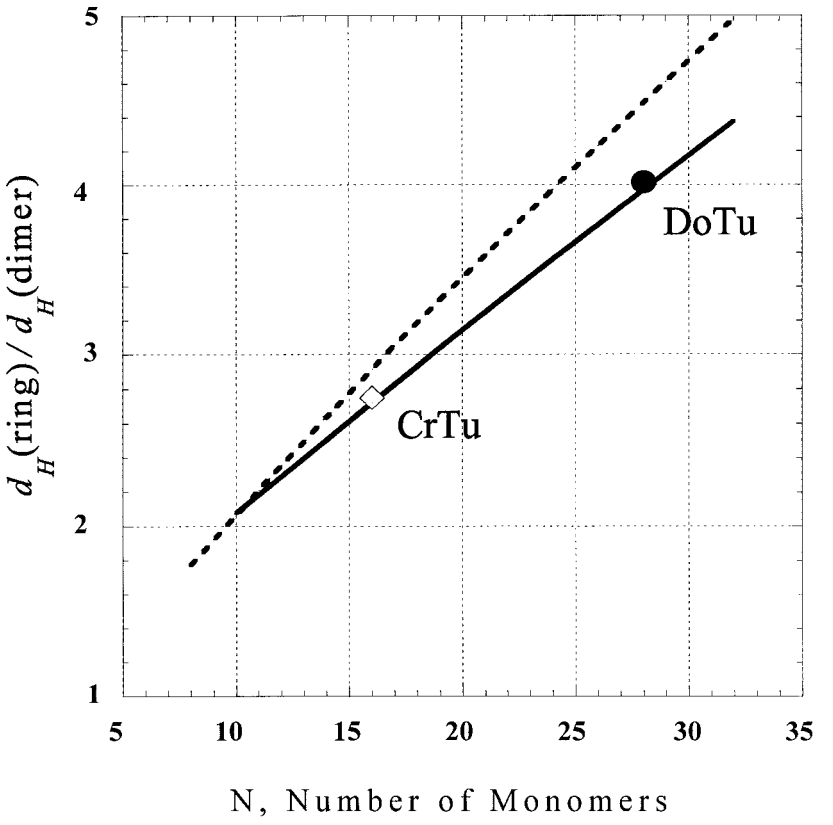

Figure 3. Calculated ratios of the hydrodynamic diameter of rings made with N monomers to the hydrodynamic diameter of isolated dimers are shown as a function of N, the number of monomers. The monomer is represented either by a spherical bead (dashed line) or 21-minibeads (solid line). The ratios derived from correlation functions measured on tubulin dimer, dolastatin-tubulin (DoTu), and cryptophycin-tubulin (CrTu) samples appear to fall close to the solid curve, indicating that the 21-minibead model is a better representation of tubulin monomers.

indicated in Reference 10. We include in Figure 3 the calculated curve of the ratios of the hydrodynamic diameters and observe the measured ratios for CrTu and DoTu rings fall close to this new curve when N is set to 16 or 28, respectively. These results are consistent with the numbers determined by electron microscopy and demonstrate that the 21-minibead monomer structure is a good model for analyzing the hydrodynamics of tubulin oligomers.

Discussion

A primary interest in FCS is its suitability for applications to solutions of nanomolar concentrations of fluorescent probes. This optical technique is relatively non-intrusive and is particularly attractive in situations involving the use of small quantities of costly or rare materials. In this study we have successfully applied FCS to investigate, in-situ, the hydrodynamic behavior of rhodamine-labeled tubulin dimers and of tubulin ring polymers induced by interactions of tubulin with cryptophycin or dolastatin. The use of ratios of diffusion times (see Figure 3) avoids the need for establishing experimental factors such as a full calibration of the illuminated volume of the FCS setup (for example, only p in Equation 2 is required from prior calibration) or for including various parameters of the sample such as solvent viscosity and temperature.

Hydrodynamic modeling and analysis of the FCS measurements on CrTu and DoTu solutions yield results consistent with those derived from electron microscopy[5] and biochemical assays[4]. Namely, the number of αβ-tubulin dimers per ring is 8 for CrTu rings and 14 for DoTu rings. It is worth noting that the unique number of tubulins per ring polymer is crucial to this analysis, and therefore it is not applicable to supramolecular structures of indefinite length such as microtubules and actin filaments. The polymerization into closed rings is driven by specific attractive interactions between the CrTu and DoTu complexes. In contrast, non-specific interactions generally lead to amorphous aggregates, which are not only difficult to reproduce experimentally, but also challenging to analyze theoretically. We have exploited the attributes of these tubulin rings to test available hydrodynamic theories of supramolecular structures. We have shown that the related calculations of hydrodynamic coefficients are quantitatively correct.

[1] B. Alberts, D. Bray, J. Lewis, M. Raff, K. Roberts, J. D. Watson, *"Molecular Biology of the Cell"* , 3rd edition, Garland Publishing, New York 1994.
[2] E. Nogales, M. Whittaker, R. A. Milligan, K. H. Downing, *Cell* **1999**, *96*, 79.
[3] C. Dumontet, B. I. Sikic, *J. Clin. Oncol.* **1999**, *17*, 1061.
[4] E. Hamel, D. G. Covell, *Curr. Med. Chem. -Anti-Cancer Agents* **2002**, *2*, 19.
[5] N. R. Watts, N. Cheng, W. West, A. C. Steven, D. L. Sackett, *Biochemistry* **2002**, *41*, 12662.
[6] H. Boukari, R. Nossal, D. Sackett, *Biochemistry* **2003**, *42* 1292.
[7] H. Boukari, V. Chernomordik, S. Krueger, R. Nossal, D. Sackett, *Physica B* **2004**, *350,* e533.
[8] H. Boukari, R. Nossal, D. Sackett, and P. Schuck, *Phys. Rev. Lett.* **2004,** *93* 98106.
[9] H. Yamakawa, J. I. Yamaki, *J. Chem. Phys.***1973**, *58*, 2049.
[10] J. F. Diaz, E. Pantos, J. Bordas, J. M. Andreu, *J. Mol. Biol.* **1994**, *238*, 214; J. G. de la Torre, J. M. Andreu, *J. Mol. Biol.* **1994**, *238*, 223
[11] W. W. Webb, *Appl. Opt.* **2001**, *40*, 3969.
[12] R. Rigler, E. S. Elson, *"Fluorescence Correlation Spectroscopy: Theory and Applications"*, Springer Series in Chemical Physics, Springer-Verlag, New York 2001.
[13] Y. Chen, J. D. M uller, K. M. Berland, E. Gratton, *Methods* **1999**, *19*, 234.
[14] S. R. Aragon, R. Pecora, *J. Chem. Phys.* **1976**, *64*, 1792.
[15] O. Krichevsky, G. Bonnet, *Rep. Prog. Phys.* **2002**, *65*, 251.
[16] K. Starchev, J. Buffle, E. P´erez, *J. Colloid Interface Sci.* **1999**, *213*, 479.
[17] J. B. Hubbard, J. F. Douglas, *Phys. Rev. E* **1993**, *47*, 2983 and references therein.
[18] J. G. de La Torre and V. A. Bloomfield, *Quarterly Rev. Biophys.* **1981**, *14*, 81.
[19] J. G. de La Torre, S. Navarro, M. C. L. Martinez, F. G. Diaz, J. L. Cascales, *Biophys. J.* **1994**, *67*, 530.